ELSEVIER

Journal of Chromatography A, 677 (1994) 151–157

JOURNAL OF CHROMATOGRAPHY A

In-line isotachophoretic focusing of very large injection volumes for capillary zone electrophoresis using a hydrodynamic counterflow

M. Mazereeuw, U.R. Tjaden*, J. van der Greef

Division of Analytical Chemistry, Leiden/Amsterdam Center for Drug Research, Leiden University, P.O. Box 9502, 2300 RA Leiden, Netherlands

First received 25 February 1994; revised manuscript received 29 March 1994

Abstract

A simple in-line isotachophoresis–capillary zone electrophoresis system for preconcentration of large sample volumes up to 25 μl is described. Model samples of $1 \cdot 10^{-4}$–$2.5 \cdot 10^{-9}$ *M* solutions of antimuscarinic drugs were used and a volumetric calibration graph over the range 2.6–20.8 μl of $1 \cdot 10^{-7}$ *M* neostigmine and propantheline was designed. The relative standard deviations of three 500-nl injections of $1 \cdot 10^{-4}$ *M* neostigmine and propantheline were 1.6 and 4.1%, respectively. Applying UV–Vis absorbance detection, concentrations in the region of 10^{-9} *M* could be detected.

1. Introduction

Capillary zone electrophoresis (CZE) is on its way to becoming an established technique in laboratories. The main reasons for this are the high separation power and ease of operation. Major drawbacks with CZE are, however, the lack of sample loadability and the low concentration sensitivity of the commonly used UV–Vis absorbance detection. Owing to the short optical path length, typically 50–100 μm, the detection limits are in the range of 10^{-6}–10^{-7} *M* [1]. Of course, the mass sensitivity is very impressive owing to the intrinsic small detection volume. Typical injection volumes in CZE are in the nanolitre range. In addition, a significant lowering of the level of interfering compounds, especially in the analysis of complex samples, is necessary. Another shortcoming of CZE is its limited selectivity. Coupling with, *e.g.*, LC pretreatment techniques seems to be essential, but places high demands on the elution volumes.

Different on-line LC and electrophoretic sample enrichment and/or clean-up techniques for CE have been described in recent years [2–18]. The electrophoretic techniques, such as ITP and field amplified injection, are based on sample stacking due to local field strength differences [7–18]. In ITP, the sample compounds are separated according to their ionic mobilities into different zones between the boundaries of a discontinuous buffer system, *i.e.*, the leading and terminating buffer. When a steady state is reached, all zones migrate with equal velocity and have distinct borders. Sharp differences in field strengths between each zone correct diffu-

* Corresponding author.

0021-9673/94/$07.00 © 1994 Elsevier Science B.V. All rights reserved
SSDI 0021-9673(94)00339-B

sion band broadening. The steady-state concentrations of the compound zones are proportional to the concentration of the leading buffer, as can be derived from the Kohlrausch equation [19]. For trace compounds this results in sample concentration.

In the "classical" electrophoresis set-up, a detection device is considered to be the last active part of the CE system and the capillary "downstream" of the detector is considered as an unimportant necessity. In coupled ITP systems, this part can be used to extend the volume of the separation system dramatically. In other words, the detector is moved up to the inlet of the capillary and is not necessarily at the end of the CE system.

Owing to the intrinsic stabilizing properties of a steady state, ITP can be performed with a hydrodynamic flow in capillaries, without loss of analyte or band broadening [19]. This also means that large volume differences and dead volumes, *e.g.*, in capillary connections, do not affect either the concentration process or a steady-state situation.

These interesting features form the basis of an extended-volume ITP–CZE system, the preliminary results of which are presented in this paper. A few characteristics of the coupled columns with different inner diameter will be discussed.

2. Experimental

2.1. Chemicals

Triethylamine >99% pure (TEA), glacial acetic acid and HPLC-grade methanol were obtained from Merck (Darmstadt, Germany) and β-alanine from Aldrich (Steinheim, Germany). The antimuscarinic drugs neostigmine hydrobromide (N) and propantheline hydrobromide (P) were purchased from Sigma (St. Louis, MO, USA). Crystal violet (CV) (Janssen Chimica, Beerse, Belgium) was used as a visible dye to follow the preconcentration process.

The leading buffer was 10 m*M* TEA solution containing 50% (v/v) methanol, adjusted to pH 5 with acetic acid. This buffer was also used as the background electrolyte in CZE. As a terminating buffer 10 m*M* β-alanine containing 50% (v/v) methanol adjusted to pH 5 with acetic acid, was used. All buffer solutions were prepared freshly every day.

Stock solutions of 10 m*M* analyte (pH 4.3) were stored at 5°C.

All solutions were prepared with water obtained from a Milli-Q system (Millipore, Bedford, MA, USA).

2.2. Apparatus

The experimental set-up is shown in Fig. 1. A programmable capillary injection system (P) (Prince, Lauerlabs, Emmen, Netherlands) suitable for siphoning and sucking was used to control the preconcentration process and the high-voltage power supply. Untreated 100 (1 and 2) and 220 μm I.D. (3), approximately 300 μm O.D., fused-silica capillaries (SGE, Ringwood, Victoria, Australia) with lengths of 60 , 10 and

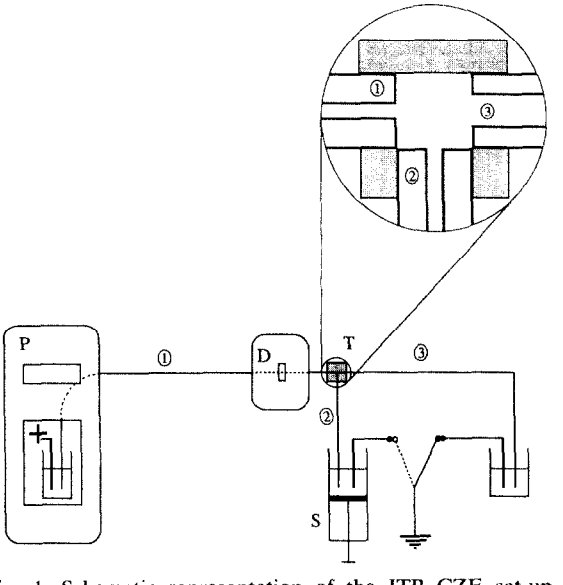

Fig. 1. Schematic representation of the ITP–CZE set-up. P = programmable capillary injection system; D = UV–Vis absorbance detector; T = laboratory-made polyethylene T-piece; S = injection syringe used as a ground electrode vessel. Untreated fused-silica capillaries of I.D. 100 μm (1 and 2) and 220 μm (3) are used.

50 cm, respectively, were connected with laboratory-made polyethylene T-piece with an internal volume of *ca.* 20 nl. A simple T-piece for low-pressure fittings was manufactured from transparent polyethylene. With a 300 μm O.D. drill, a T-shaped channel was created in which the three fused-silica tubes were inserted.

The outlet of capillary 2 (see Fig. 1) could be (de)blocked manually by means of a septum. The septum was positioned on the plunger of an injection syringe (S) used as an electrode vessel. Next to the outlet of the syringe a large opening was created for the ground electrode and to avoid any inducement of pressure differences. Capillary 2 was mounted on the syringe by means of a fingertight–union combination and (de)-blocked by moving the plunger.

Three leveled electrode vials with two ground electrodes and an anode were used. During the switch-over from ITP to CZE the ground electrode connections were changed.

Detection at 200 nm was performed on the 100 μm I.D. capillary (1) at 50 mm from the T-piece using a Spectra 100 UV–Vis absorbance detector (D) (Spectra-Physics, Mount View, CA, USA) at a wavelength of 200 nm. The signal was registered on a Model 40 flat-bed recorder (Kipp & Zonen, Delft, Netherlands).

2.3. ITP–CZE procedure

The ITP–CZE procedure as developed by Reinhoud *et al.* [12] was modified and is shown schematically in Fig. 2. In step A the total capillary system is filled with leading buffer, which is also used as the CZE background electrolyte. The outlet of capillary 2 (see Fig. 1) is closed and the capillary is loaded with sample, dissolved in terminating buffer. In the following step B, the sample vial is replaced with the anode vial containing terminating buffer and the ITP process is initially started at +10 kV, decreased to +7 kV after 1 h. To compensate for the electroosmotic flow (EOF) and to move back the preconcentrated sample zone to the capillary inlet during the ITP process, a hydrodynamic counterflow is applied. After focusing and moving back the sample zone simultaneously for

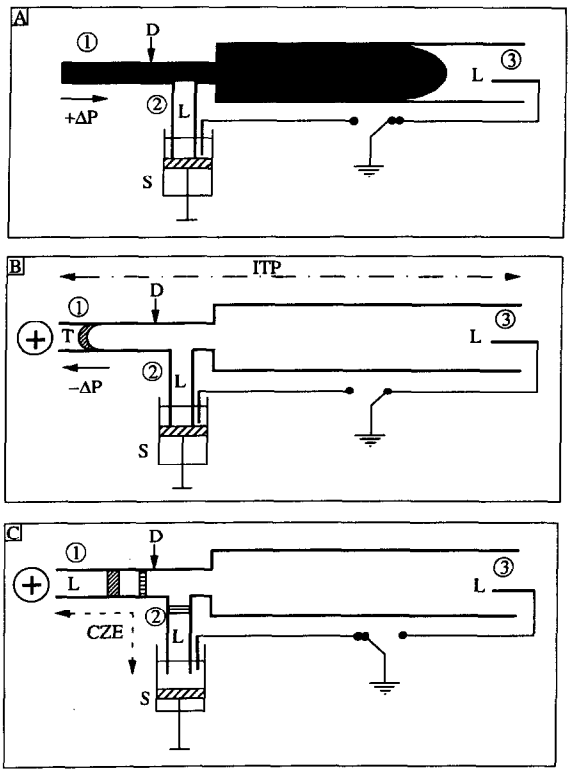

Fig. 2. Schematic representation of the ITP–CZE procedure in three steps (A, B and C). The focusing step is performed between the terminating (T) and leading (L) buffers in capillaries 1 and 3 and controlled with a pressure difference ΔP. Capillary 2 can be (de)blocked by means of the syringe vessel S. D = detection device.

5–150 min depending on the volume of analyte injected, the visible marker crystal violet, which has the lowest mobility (see Fig. 4a), reaches the inlet of the capillary. Then, in the final step C, the terminating buffer vial is replaced with a leading buffer-containing vial, the electrodes are exchanged, capillary 2 deblocked and CZE is started and performed at +30 kV.

3. Results and discussion

Concentrating a large volume takes a relatively long time, mainly depending on the applied field strength, the migration path length and the mobility of the compounds. Therefore,

increasing the diameter of the preconcentration system is preferred to increasing the capillary length. In the latter instance, the sample volume is only increased linearly by changing the length, while the diameter affects the volume according to the square root, which makes shorter capillaries, *i.e.*, migration path length, and a high electric field strength possible. Unfortunately, Joule heating plays a more prominent role in wide-bore capillaries. An optimum compromise between the focusing time and diameter has to be found. Coupling of columns with different inner diameters results in inhomogeneous electrophoretic conditions, *e.g.*, the electric field strength, which are considered in this section.

The ITP channel consisted in fact of two capillaries with different inner diameters, which can be considered as a series combination of two resistors, R_1 and R_2. For a capillary with length L (cm), the electric resistor R (S^{-1}) can be defined as

$$R = \frac{4L}{\pi d^2 \kappa} \tag{1}$$

were d is the inner diameter of the capillary (cm) and κ the specific conductivity (S cm^{-1}) of the electrolyte. If the current I is considered to be constant, the ratio of the field strengths over two coupled capillaries (E_1/E_2) can be expressed by the equation

$$\frac{E_1}{E_2} = \frac{d_2^2}{d_1^2} \cdot \frac{\kappa_2}{\kappa_1} \tag{2}$$

The EOF volume throughput, Φ_{eof}(μl min^{-1}), can be calculated from

$$\Phi_{eof} = v_{eof} \cdot \frac{\pi d^2}{4} \tag{3}$$

where v_{eof} is the EOF flow-rate (mm min^{-1}), which can be expressed as

$$v_{eof} = \mu_{eof} E \tag{4}$$

where μ_{eof} represents the electroosmotic mobility (mm^2 min^{-1} V^{-1}). Combining Eqs. 2, 3 and 4 demonstrates that the ratio of the EOF volume throughput in the two capillaries ($\Phi_{1,eof}/\Phi_{2,eof}$) is independent of the capillary diameters and

$$\frac{\Phi_{1,eof}}{\Phi_{2,eof}} = \frac{\mu_{eof}}{\mu_{eof}} \cdot \frac{d_2^2}{d_1^2} \cdot \frac{\kappa_2}{\kappa_1} \cdot \frac{4\pi d_1^2}{4\pi d_2^2} = 1 \tag{5}$$

for a continuous buffer system ($\kappa_2/\kappa_1 = 1$), neglecting the influence of Joule heating, and can therefore be equally compensated over the coupled capillaries by means of a hydrodynamic counterflow. Thus no pressure build-up is generated in the capillary connection which can disturb the preconcentration or steady state.

However, Eq. 2 shows that the EOF cannot be considered constant in a discontinuous buffer system because of the differences in conductivity. Further, the field strength differences and hence the differences in migration rate will be strongly dependent on the choices of the inner diameters. As a consequence, the preconcentration time in the wide-bore capillary, compared with the small-bore part, will increase significantly with increase in capillary diameter.

In Table 1 the set-up shown in Fig. 1 is compared with a set-up in which the volume extension is achieved by using a long small-bore capillary and a homogeneous field strength is present. A continuous background electrolyte was considered. As can be seen, the field strengths in both extension capillaries are similar. As the electrophoretic velocity is proportional to the field strength (Eq. 4), the migration time and hence the focusing time in system II will be approximately five times longer than in system I. Therefore, a short wide-bore capillary is to be preferred above a long small-bore capillary with the same inner volume.

Another consequence of coupling capillaries

Table 1
Comparison of two extended volume systems with different inner diameters

Parameter	System I	System II
Total volume (μl)	23.7	23.7
Inner diameter (1) (μm)	100	100
Inner diameter (3) (μm)	220	100
Length (1) (m)	0.6	0.6
Length (3) (m)	0.5	2.42
Electric field strength (kV m^{-1})	3.4[a]	3.3

[a] Calculated according to Eq. 2.

with different inner diameters is the difference in EOF due to the unequal heat dissipation ΔT, proportional to the square of the inner diameter [20]:

$$\Delta T = \frac{Qd^2}{16\lambda} \quad (6)$$

where Q is the heat generated (λ cm^{-3} K^{-1}) and λ is the thermal conductance (W cm^{-1} K^{-1}). This can result in a pressure build-up which can disturb the flow profile, especially in the T-piece section. Therefore, we constructed an Ohm's law plot (Fig. 3) to calculate the maximum voltage at which the curve begins to deviate from linearity. The voltage was *ca.* +15 kV. In this study a voltage of +10 kV was applied. Although application of higher field strengths results in shorter focusing times, perturbation of the ITP process may occur.

The T-piece does not contribute significantly to the EOF, owing to the low zeta potential in comparison with fused silica and a sharp bend (90°C) being present in the CZE channel. As a consequence, a small pressure build-up, depending on the length of the non-contributing part, will exist and possibly influence the efficiency during the CZE step. However, comparison of CZE separations without and with the T-piece (Fig. 4a and b) shows no significant differences in efficiency.

Owing to the self-regulating properties of a

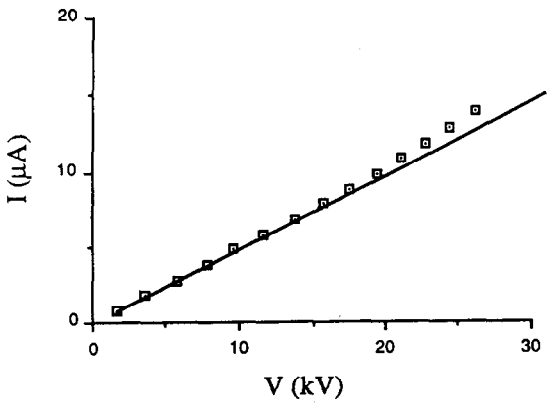

Fig. 3. Ohm's law plot for leading buffer in the coupled 100 and 220 μm I.D. capillaries. A small deviation from the ideal line, due to Joule heating, is present.

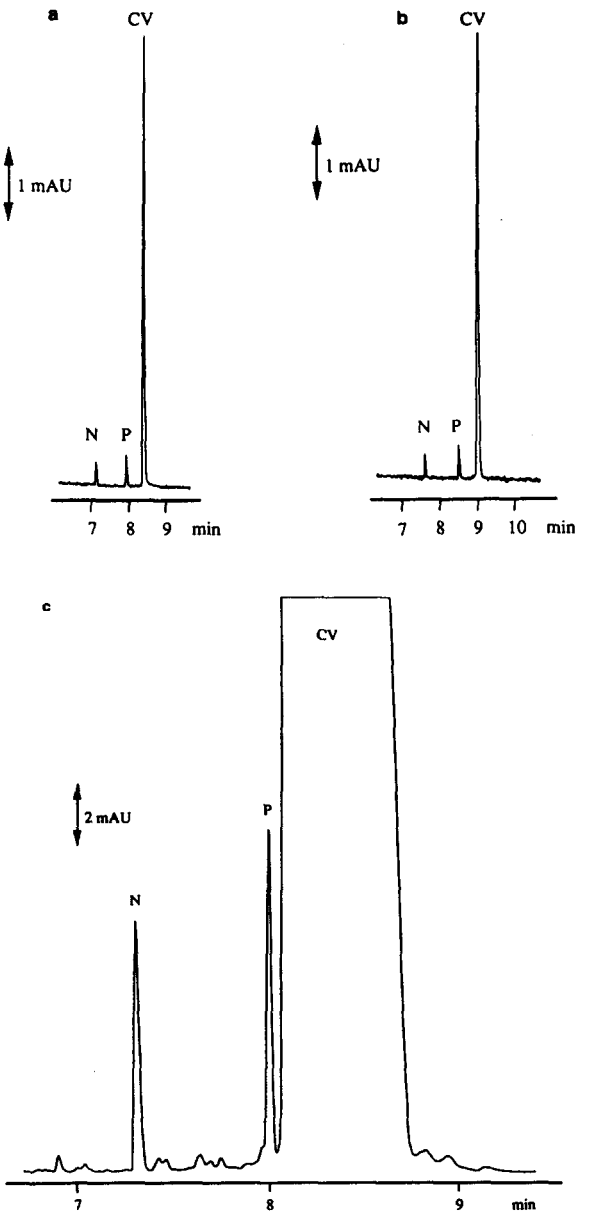

Fig. 4. Electropherograms for a 128-nl injection, (a) without and (b) with a T-piece, of $1 \cdot 10^{-6}$ *M* neostigmine (N) and propantheline (P) and $1 \cdot 10^{-5}$ *M* crystal violet (CV), (c) ITP–CZE of a 20.8-μl sample of $1 \cdot 10^{-7}$ *M* N and P and $1 \cdot 10^{-5}$ *M* CV as a visual marker. The ITP step is performed for 2.5 h using +10 kV initially, lowered to +7 kV after 1 h. The hydrodynamic counterflow is induced by a −30 mbar pressure at the capillary inlet. All samples are dissolved in terminating buffer. The CZE is performed in leading buffer using a field strength of 400 V cm^{-1} (10.6 μA). The ITP–CZE procedure is described under Experimental.

steady state in ITP, the focusing time can theoretically be infinitely long without analyte loss or band broadening and capillary connections with a relatively large dead volume, as present in our system, are applicable. Limitations to the hydrodynamic flow rate are determined by the extent in which a steady state is able to stabilize itself. Extreme conditions, *i.e.*, a strong electroosmotic flow induced by a high field strength, that is compensated by a strong counterflow, will disturb the focusing process and the steady state and, consequently, analyte loss will occur. An optimum compromise between focusing time and conditions has to be found.

3.1. Quantitative aspects

In Fig. 4b and c a comparison is made between 128 nl of $1 \cdot 10^{-6}$ *M* N and P without ITP preconcentration and 20.8 μl of $1 \cdot 10^{-7}$ *M* N and P after ITP focusing. It can be easily seen that a dramatic increase in the detection signal was obtained. The concentration of CV in both samples was $1 \cdot 10^{-5}$ *M*. Although the preconcentration step took *ca.* 2.5 h, high efficiency and good resolution were still achieved.

The relative standard deviation of the peak areas with three 500-nl injections of $1 \cdot 10^{-4}$ *M* N, P and CV were 1.6, 4.1 and 1.7% respectively. The loading procedure was found to be satisfactorily linear over the range 2.6–20.8 μl of sample solution. The plots of peak area and height *versus* the volumes of N and P were given by the equations $y = 0.064(\pm 0.001)x + 0.02(\pm 0.01)$ ($r^2 = 0.9997$, $n = 4$) and $y = 0.090(\pm 0.004)x - 0.01(\pm 0.05)$ ($r^2 = 0.9975$, $n = 4$), respectively, were y is in area units and x in μl. Peak areas give better results than peak heights. This can be explained by the fact that diffusion has a relatively larger influence on short than long sample plugs during the CZE step.

As there is basically no limitation on the injection volume, detection limits are determined by the amount of background signal caused by impurities in, *e.g.*, the buffer system or solvents, and the available analysis time. Fig. 5 shows the signal after focusing 20.8 μl of $2.5 \cdot 10^{-9}$ *M* N, and *P* and $2.5 \cdot 10^{-6}$ *M* CV.

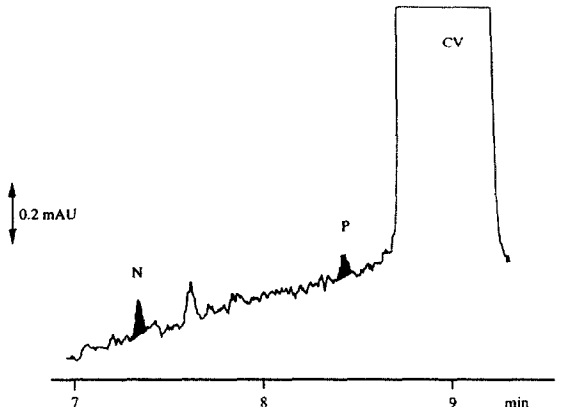

Fig. 5. ITP–CZE of a 20.8-μl sample of $2.5 \cdot 10^{-9}$ *M* neostigmine (N) and propantheline (P) and $2.5 \cdot 10^{-6}$ *M* crystal violet (CV) as a visual marker. Experimental conditions as in Fig. 4.

A larger sample volume and more selective detection will improve the detection limit.

4. Conclusions

Large sample volumes of up to 20.8 μl of $1 \cdot 10^{-7}$ *M*, N and P can be preconcentrated using ITP and easily detected with UV–Vis absorbance detection. However, a long focusing time was required. The relative standard deviations of the peak areas for three 500-nl $1 \cdot 10^{-4}$ *M* N, P and CV injections were in the range 1.6–4.1%. Detection limits are determined by the amount of impurities that mask the analyte signal and the available analysis time, but $2.5 \cdot 10^{-9}$ *M* N and P could be detected. Optimization and improvement of the injection volume, determination limit, analysis time and applications are under investigation.

5. References

[1] S.F.Y. Li, *Capillary Electrophoresis: Principles, Practice and Applications*, Elsevier, New York, 1992.
[2] N.A. Guzman, M.A. Trebilcock and H.P. Advis, *J. Liq. Chromatogr.*, 14 (1991) 997.

[3] A.J.J. Debets, M. Mazereeuw, W.H. Voogt, D.J. van Iperen, H. Lingeman, K.-P. Hupe and U.A.Th. Brinkman, *J. Chromatogr.*, 608 (1992) 151.
[4] M.M. Bushey and J.W. Jorgenson, *Anal. Chem.*, 62 (1990) 978.
[5] J. Cai and Z. El Rassi, *J. Liq. Chromatogr.*, 15 (1992) 1179.
[6] F. Foret, V. Sustacek and P. Bocek, *J. Microcol. Sep.*, 2 (1990) 229.
[7] D.S. Stegehuis, U.R. Tjaden and J. van der Greef, *J. Chromatogr.*, 591 (1992) 341.
[8] D.S. Stegehuis, H. Irth, U.R. Tjaden and J. van der Greef, *J. Chromatogr.*, 538 (1992) 393.
[9] D. Kaniansky and J. Marak, *J. Chromatogr.*, 498 (1990) 191.
[10] V. Dolnik, K.A. Cobb and Novotny, *J. Microcol. Sep.*, 2 (1990) 127.
[11] N.J. Reinhoud, U.R. Tjaden and J. van der Greef, *J. Chromatogr.*, 641 (1993) 155.
[12] N.J. Reinhoud, U.R. Tjaden and J. van der Greef, *J. Chromatogr. A*, 653 (1993) 303.
[13] R.L. Chien and D.S. Burgi, *Anal. Chem.*, 64 (1992) A489.
[14] F. Foret, E. Szoko and B.L. Karger, *J. Chromatogr.*, 608 (1992) 3.
[15] R.L. Chien and D.S. Burgi, *Anal. Chem.*, 64 (1992) 1046.
[16] D.S. Burgi and R.L. Chien, *Anal. Chem.*, 63 (1991) 2042.
[17] C. Schwer and F. Lottspeich, *J. Chromatogr.*, 623 (1992) 345.
[18] F.E.P. Mikkers, F.M. Everaerts and T.P.E.M. Verheggen, *J. Chromatogr.*, 169 (1979) 11.
[19] F.M. Everaerts, J.L. Beckers and T.P.E.M. Verheggen, *Isotachophoresis: Theory, Instrumentation and Practice*, Elsevier, Amsterdam, 1976.
[20] J.H. Knox, *Chromatographia*, 26 (1988) 329.